THE JOURNAL OF PHYSICAL CHEMISTRY C

Article

pubs.acs.org/JPCC

Improvement of Nb Doping on SO_2 Resistance of VO_x/CeO_2 Catalyst for the Selective Catalytic Reduction of NO_x with NH_3

Zhihua Lian,[†,‡] Fudong Liu,[§,∥] Wenpo Shan,[†,‡] and Hong He*[,†,‡,§]

[†]Center for Excellence in Regional Atmospheric Environment and [‡]Key Laboratory of Urban Pollutant Conversion, Institute of Urban Environment, Chinese Academy of Sciences, Xiamen 361021, China

[§]Research Center for Eco-Environmental Sciences, Chinese Academy of Sciences, Beijing 100085, China

Supporting Information

ABSTRACT: The influence of sulfation treatment on Nb−VO_x/CeO_2 and VO_x/CeO_2 catalysts for the selective catalytic reduction (SCR) of NO_x with NH_3 was fully investigated. The Nb−VO_x/CeO_2 catalyst showed higher catalytic activity and stronger resistance to SO_2 than VO_x/CeO_2. The formation of sulfates, small specific surface area, and reduction in the number of active sites were all responsible for the low catalytic activity over VO_x/CeO_2 after sulfation under SCR conditions. On the contrary, Nb−VO_x/CeO_2 adsorbed much more nitrate than sulfate when sulfated under SCR conditions and showed much higher NH_3-SCR activity than VO_x/CeO_2 after the same treatment. After sulfation by $SO_2 + O_2$ only, instead of sulfation under SCR conditions, both of the samples exhibited decreased NH_3-SCR activity, mainly due to the formation of sulfates and the blockage of the Langmuir−Hinshelwood reaction pathway.

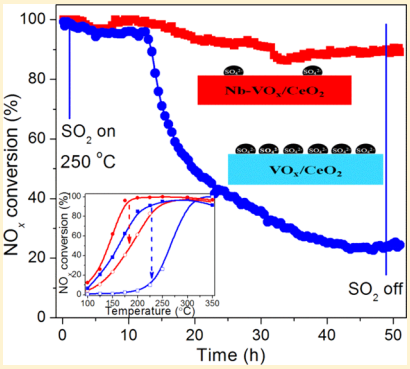

1. INTRODUCTION

Nitrogen oxides (NO and NO_2), as major air pollutants, result from industrial combustion of fossil fuels and automobile exhaust gas.[1] They contribute to a variety of environmentally harmful effects, such as photochemical smog, acid rain, and haze.[2] The selective catalytic reduction of NO_x with NH_3 (NH_3-SCR) over V_2O_5−$WO_3(MoO_3)/TiO_2$ is a well proven technique for the removal of nitrogen oxides.[3−6] However, some disadvantages remain for the present vanadium-based catalyst, such as a relatively narrow operating temperature window of 300−400 °C and low N_2 selectivity at high temperatures.[7−10] Therefore, there has been strong interest in developing novel vanadium catalysts with high activity and high N_2 selectivity.

Typical coal- and diesel-fired exhausts usually contain varying amounts of SO_2. During long-term SCR operation, even a small amount of SO_2 can deactivate the catalysts due to the formation of metal sulfate species, the blockage of catalyst pore channels, and/or the cutting off of the redox cycle of active phases.[11−13] For example, the chemical transformation of MnO to $MnSO_4$ was found to be the main reason for the deactivation of the SCR over MnO_x.[14] Ammonium bisulfate (NH_4HSO_4) accumulated on the surface of V_2O_5/TiO_2 and interfered with the SCR reaction.[15] Therefore, it is important to investigate the influence of sulfation on the structure and activity of catalysts, which will be beneficial for understanding the deactivation mechanism and further improvement of the SO_2 durability.

In our previous study, we demonstrated that VO_x/CeO_2 prepared by the homogeneous precipitation method possesses higher NH_3-SCR activity than that prepared by other preparation methods and that the addition of Nb could significantly promote the SCR activity of the VO_x/CeO_2 catalyst, especially in the low temperature range.[16,17] The Nb−VO_x/CeO_2 catalyst presented more acid sites owing to the addition of niobium oxide. The interaction of V, Ce, and Nb resulted in better dispersion of vanadium species and stronger redox capability at low temperatures. Both of these factors were responsible for more favorable NH_3-SCR performance over Nb−VO_x/CeO_2.

In this study, the influence of sulfation under SCR atmosphere and sulfation by $SO_2 + O_2$ only on Nb−VO_x/CeO_2 and VO_x/CeO_2 catalysts was studied in detail. Brunauer−Emmett−Teller (BET) analysis, H_2 temperature-programmed reduction (H_2-TPR), X-ray photoelectron spectroscopy (XPS), and in situ diffuse reflectance infrared Fourier transform spectroscopy (in situ DRIFTS) were used to characterize the sulfated samples. After the treatment, a large amount of sulfate species formed on Nb−VO_x/CeO_2−sulfation by $SO_2 + O_2$ only, VO_x/CeO_2−sulfation by $SO_2 + O_2$ only, and VO_x/CeO_2−sulfation under SCR conditions, leading to low NH_3-SCR catalytic activity. However, only a much smaller amount of sulfate species was detected on Nb−VO_x/CeO_2−sulfation under SCR conditions, and thus higher catalytic activity was obtained.

Received: December 20, 2016
Revised: March 20, 2017
Published: March 21, 2017

DOI: 10.1021/acs.jpcc.6b12772
J. Phys. Chem. C 2017, 121, 7803−7809

2. EXPERIMENTAL SECTION

2.1. Catalyst Synthesis and Activity Tests. The VO_x/CeO_2 (mass ratio of vanadium oxide 1 wt %) and $Nb-VO_x/CeO_2$ (mass ratio of NbO_x 30 wt %) catalysts were prepared by a homogeneous precipitation method. The preparation procedures have been described in detail in our previous studies.[16] In the present study, sulfated catalysts were obtained by pretreating $Nb-VO_x/CeO_2$ and VO_x/CeO_2 in a flow of 500 ppm of NH_3 + 500 ppm of NO + 5 vol % O_2 + 100 ppm of SO_2 (catalyst-sulfation under SCR conditions) or 100 ppm of SO_2 + 5 vol % O_2 (catalyst-sulfation by SO_2 + O_2 only) at 250 °C for 48 h. The medium temperature 250 °C was selected due to high activity and the literature references.[18,19]

Before NH_3-SCR activity tests, the catalysts were pressed, crushed, and sieved to 40−60 mesh. The SCR activity tests were carried out in a fixed-bed quartz flow reactor at atmospheric pressure. The reaction conditions were controlled as follows: 500 ppm of NO, 500 ppm of NH_3, 5 vol % O_2, 100 ppm of SO_2 (when used), and N_2 as the balance. Under ambient conditions, the total flow rate was 500 mL/min and the gas hourly space velocity (GHSV) was 50 000 h^{-1}. The amount of catalysts used in activity tests was 0.6 mL (about 0.7 g). The effluent gas, including NO, NH_3, NO_2, and N_2O, was continuously analyzed by an FTIR spectrometer (Nicole Nexus 670) equipped with a heated, low-volume multiple-path gas cell (2 m). The FTIR spectra were collected after the SCR reaction had reached a steady state, and the NO_x conversion and N_2 selectivity were calculated as follows:

$$NO_x \text{ conversion} = \left(1 - \frac{[NO]_{out} + [NO_2]_{out}}{[NO]_{in} + [NO_2]_{in}}\right) \times 100\% \quad (1)$$

$$N_2 \text{ selectivity} = \frac{[NO]_{in} + [NH_3]_{in} - [NO_2]_{out} - 2[N_2O]_{out}}{[NO]_{in} + [NH_3]_{in}} \times 100\% \quad (2)$$

2.2. Characterization of the Catalysts. The surface area and pore characteristics of the catalysts were obtained from N_2 adsorption/desorption analysis at −196 °C using a Quantachrome Quadrasorb SI-MP. Prior to the N_2 physisorption, the catalysts were degassed at 300 °C for 5 h. Surface area was determined by the BET equation in the 0.05−0.35 partial pressure range. Pore volume and average pore diameter were determined by the Barrett−Joyner−Halenda (BJH) method from the desorption branches of the isotherms.

The H_2-TPR experiments were carried out on a Micromeritics Auto Chem 2920 chemisorption analyzer. The samples (30 mg) were pretreated at 300 °C in a flow of 20 vol % O_2/Ar (50 mL/min) for 0.5 h in a quartz reactor and cooled down to room temperature (30 °C) followed by Ar purging for 0.5 h. A 50 mL/min gas flow of 10% H_2 in Ar was then passed over the samples through a cold trap to the detector. The reduction temperature was raised from 30 to 1000 °C at 10 °C min^{-1}.

X-ray photoelectron spectroscopy (XPS) spectra of the catalysts were recorded on a scanning X-ray microprobe (Axis Ultra, Kratos Analytical Ltd.) using Al Kα radiation (1486.7 eV). All the binding energies were calibrated using the C 1s peak (BE = 284.8 eV) as standard.

2.3. In Situ DRIFTS Studies. In situ DRIFTS experiments were performed on an FTIR spectrometer (Nicolet Nexus 670) equipped with a Smart Collector and an MCT/A detector cooled by liquid nitrogen. The reaction temperature was controlled precisely by an Omega programmable temperature controller. Prior to each experiment, the sample was pretreated at 300 °C for 0.5 h in a flow of 20 vol % O_2/N_2 and then cooled down to 175 °C. The background spectra were collected in flowing N_2 and automatically subtracted from the sample spectrum. The reaction conditions were controlled as follows: 300 mL/min total flow rate, 500 ppm of NH_3 and/or 500 ppm of NO, 100 ppm of SO_2 (when used), 5 vol % O_2, and N_2 as the balance. All spectra were recorded by accumulating 100 scans with a resolution of 4 cm^{-1}.

3. RESULTS

3.1. Catalytic Activity. Figure 1 exhibits the effect of SO_2 on the catalytic activity over $Nb-VO_x/CeO_2$ and VO_x/CeO_2 catalysts at 250 °C. When 100 ppm of SO_2 was introduced into the inlet gas, the NO_x conversion over VO_x/CeO_2 decreased from 100% to 24% in 48 h and could not recover to the initial activity after the removal of SO_2, which indicates that the inhibiting effect of SO_2 on the SCR activity over the VO_x/CeO_2 catalyst was severe and irreversible. However, the SO_2 effect on $Nb-VO_x/CeO_2$ was quite different. The NO_x conversion decreased slightly, and nearly 90% NO_x conversion could still be obtained in the presence of 100 ppm of SO_2 for a 48 h test. After the SO_2 was cut off, the activity over $Nb-VO_x/CeO_2$ could not be restored to the original level. Both of the catalysts showed high N_2 selectivity. The NO_x conversion in 300 ppm of SO_2 [Figure S1, Supporting Information (SI)] decreased more seriously than that in 100 ppm of SO_2. However, the $Nb-VO_x/CeO_2$ catalyst still presented much stronger resistance to SO_2 than VO_x/CeO_2.

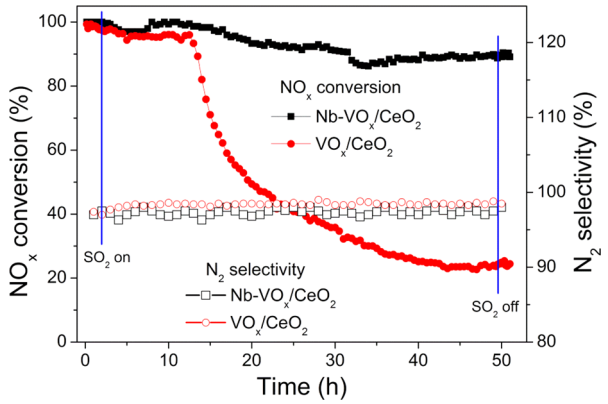

Figure 1. Effect of SO_2 on SCR activity over VO_x/CeO_2 and $Nb-VO_x/CeO_2$ catalysts at 250 °C. Reaction conditions: [NO] = [NH_3] = 500 ppm, [SO_2] = 100 ppm (when used), [O_2] = 5 vol %, N_2 as the balance, total flow rate 500 mL/min, and GHSV = 50 000 h^{-1}.

The NH_3-SCR activity over the fresh and sulfated $Nb-VO_x/CeO_2$ and VO_x/CeO_2 catalysts is shown in Figure 2. $Nb-VO_x/CeO_2$ presented higher NO_x conversion than VO_x/CeO_2, especially in the temperature range of 150−250 °C. At 175 °C, the NO_x conversion over $Nb-VO_x/CeO_2$ and VO_x/CeO_2 was 95% and 60%, respectively. The addition of Nb to VO_x/CeO_2 enhanced the NH_3-SCR activity. The NO_x conversion over $Nb-VO_x/CeO_2$ was higher than that over Nb/CeO_2 (Figure S2, SI). N_2 selectivity over these catalysts was above 90%, as shown in Figure S3 (SI).

DOI: 10.1021/acs.jpcc.6b12772
J. Phys. Chem. C 2017, 121, 7803−7809

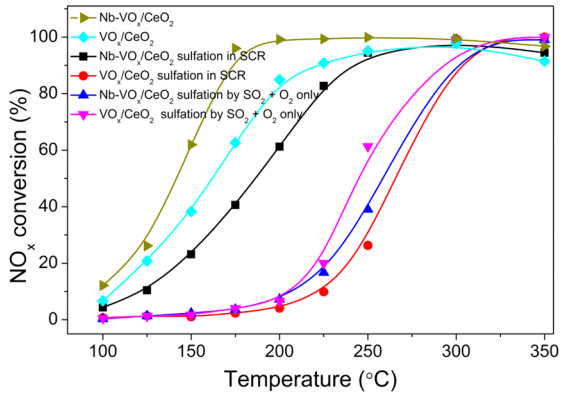

Figure 2. NH_3-SCR activity over the fresh and sulfated Nb−VO_x/CeO_2 and VO_x/CeO_2 catalysts. Reaction conditions: [NO] = [NH_3] = 500 ppm, [O_2] = 5 vol %, N_2 as the balance, total flow rate 500 mL min^{-1}, and GHSV = 50 000 h^{-1}.

After sulfation under SCR atmosphere, the catalytic activity over Nb−VO_x/CeO_2 and VO_x/CeO_2 catalysts decreased to some extent, compared to that of the fresh catalysts. However, the Nb−VO_x/CeO_2 catalyst still exhibited much better catalytic performance than the VO_x/CeO_2 catalyst; 80% and 10% NO_x conversion was obtained at 225 °C over Nb−VO_x/CeO_2−sulfation under SCR conditions and VO_x/CeO_2−sulfation under SCR conditions, respectively. Nb−VO_x/CeO_2−sulfation by SO_2 + O_2 only and VO_x/CeO_2−sulfation by SO_2 + O_2 only both exhibited low SCR activity, similar to VO_x/CeO_2−sulfation under SCR conditions. Among these four sulfation samples, Nb−VO_x/CeO_2−sulfation under SCR conditions showed the highest NH_3-SCR activity; the reasons for this will be discussed later.

3.2. Catalyst Characterization. The surface area and pore characteristics of VO_x/CeO_2 and Nb−VO_x/CeO_2 catalysts before and after SO_2 poisoning are shown in Table 1. The fresh

Table 1. N_2 Physisorption Results for VO_x/CeO_2 and Nb−VO_x/CeO_2 Catalysts before and after SO_2 Poisoning

catalysts	specific surface area (m^2/g)	pore diameter (nm)	pore volume (cm^3/g)
Nb−VO_x/CeO_2	168.2	3.5	0.15
Nb−VO_x/CeO_2−sulfation under SCR conditions	135.3	7.1	0.24
Nb−VO_x/CeO_2−sulfation by SO_2 + O_2 only	15.5	12.2	0.05
VO_x/CeO_2	131.3	3.5	0.12
VO_x/CeO_2−sulfation under SCR conditions	15.5	26.1	0.10
VO_x/CeO_2−sulfation by SO_2 + O_2 only	18.2	15.4	0.07

Nb−VO_x/CeO_2 catalyst presented a slightly larger specific surface area and pore volume than VO_x/CeO_2. After sulfation under SCR conditions, the specific surface area of the VO_x/CeO_2 catalyst decreased significantly, while the Nb-modified catalyst did not change much. The specific surface area of Nb−VO_x/CeO_2−sulfation under SCR conditions was 135.3 m^2/g. However, after sulfation by SO_2 + O_2 only, the structural parameters over both of the catalysts changed remarkably. The specific surface area of the VO_x/CeO_2 sample decreased from 131.3 to 18.2 m^2/g and the average pore diameter increased from 3.5 to 15.4 nm after sulfation by SO_2 + O_2 only. In summary, Nb−VO_x/CeO_2−sulfation by SO_2 + O_2 only, VO_x/CeO_2−sulfation by SO_2 + O_2 only, and VO_x/CeO_2−sulfation under SCR conditions all showed much smaller specific surface area than the fresh catalysts, while only Nb−VO_x/CeO_2−sulfation in SCR still exhibited a large specific surface area.

H_2-TPR results over the fresh and sulfated Nb−VO_x/CeO_2 and VO_x/CeO_2 samples are presented in Figure 3. A distinctive

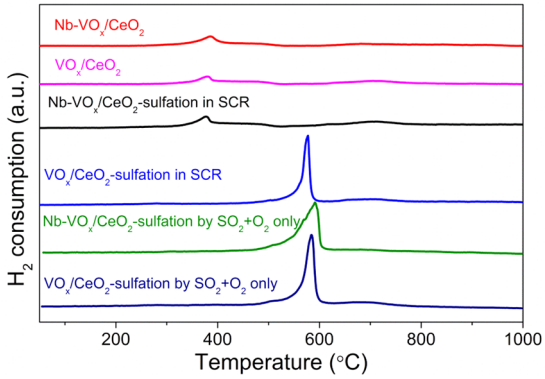

Figure 3. H_2-TPR results over the fresh and sulfated Nb−VO_x/CeO_2 and VO_x/CeO_2 samples.

H_2 reduction peak at about 580 °C was observed over VO_x/CeO_2−sulfation under SCR conditions, Nb−VO_x/CeO_2−sulfation by SO_2 + O_2 only, and VO_x/CeO_2−sulfation by SO_2 + O_2 only, which was assigned to the reduction of sulfate.[20,21] This indicates that there was a substantial amount of sulfate deposited on these three samples. However, the H_2-TPR profile over Nb−VO_x/CeO_2−sulfation under SCR conditions was similar to that of fresh Nb−VO_x/CeO_2, demonstrating that there was almost no sulfate formed on the sample.

Figure 4 exhibits the XPS results of S 2p on Nb−VO_x/CeO_2 and VO_x/CeO_2 samples after sulfation under SCR conditions

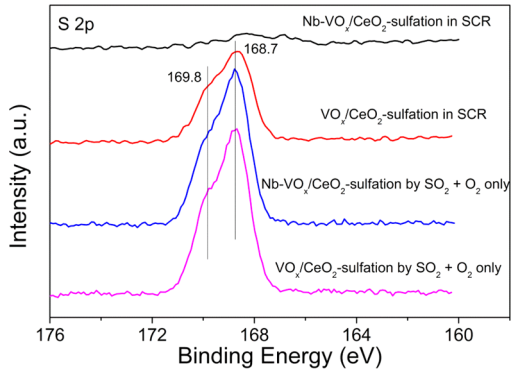

Figure 4. XPS results of S 2p on Nb−VO_x/CeO_2 and VO_x/CeO_2 samples after sulfation under SCR conditions and sulfation by SO_2 + O_2 only.

and sulfation by SO_2 + O_2 only. Two prominent peaks attributed to S 2p were observed on VO_x/CeO_2−sulfation under SCR conditions, Nb−VO_x/CeO_2−sulfation by SO_2 + O_2 only, and VO_x/CeO_2−sulfation by SO_2 + O_2 only, implying the formation of sulfur-containing species on the catalyst surface. The S 2p peaks were mainly centered at 168.7 and 169.8 eV and could be assigned to SO_4^{2-} and HSO_4^-, respectively.[22−24] However, a much smaller S 2p peak was detected on Nb−VO_x/

DOI: 10.1021/acs.jpcc.6b12772
J. Phys. Chem. C 2017, 121, 7803−7809

CeO_2–sulfation under SCR conditions, indicating that the amount of sulfate accumulated on this sample is insignificant, which is in good accordance with the H_2-TPR results.

Figure S4 (SI) showed NH_3-TPD results of Nb–VO_x/CeO_2 and VO_x/CeO_2 samples after sulfation under SCR conditions. The adsorption amount of NH_3 over Nb–VO_x/CeO_2–sulfation in SCR was much larger than that over VO_x/CeO_2–sulfation in SCR, which may be related to the specific surface area. NO-TPD results of Nb–VO_x/CeO_2 and VO_x/CeO_2 samples after sulfation under SCR conditions were presented in Figure S5 (SI). VO_x/CeO_2–sulfation in SCR showed no NO adsorption, while Nb–VO_x/CeO_2–sulfation in SCR still showed a small adsorption amount of NO. The adsorption of NO on VO_x/CeO_2–sulfation in SCR was inhibited due to the formation of sulfate and the small specific surface area.

3.3. In Situ DRIFTS. To demonstrate the difference between Nb–VO_x/CeO_2 and VO_x/CeO_2 further, the in situ DRIFTS technique was used. First, NO + NH_3 + O_2 were fully adsorbed on the surface of Nb–VO_x/CeO_2 and VO_x/CeO_2 for 60 min at 250 °C. Then, the background spectra were collected and automatically subtracted from the sample spectrum. Finally, SO_2 was introduced into the SCR reaction system, and the results are shown in Figure 5. Several bands appeared, including

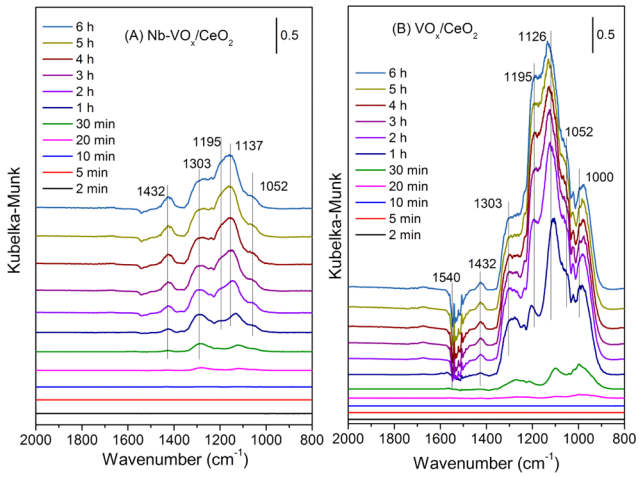

Figure 5. DRIFT spectra of SO_2 adsorption on Nb–VO_x/CeO_2 (A) and VO_x/CeO_2 (B) catalysts under the SCR conditions (500 ppm of NH_3 + 500 ppm of NO + 5 vol % O_2) at 250 °C.

those for ionic NH_4^+ on Brønsted acid sites (1432 cm^{-1})[16,25] and sulfate species (1303, 1205, 1137, 1052, and 1000 cm^{-1}).[26−29] Nitrate consumption bands at 1540 cm^{-1}[16,30] also appeared, indicating that the nitrate species was displaced by the formation of sulfate on VO_x/CeO_2. In the sulfation process, SO_2 could react with metal cations, consuming a number of Lewis acid sites and could form Brønsted acid sites due to the formation of S–OH.[31,32] Therefore, the bands at 1432 cm^{-1} were observed. It is evident that the amount of sulfate species on VO_x/CeO_2 was much larger than that on Nb–VO_x/CeO_2, which was consistent with the XPS results of Nb–VO_x/CeO_2–sulfation in SCR and VO_x/CeO_2–sulfation in SCR.

To investigate the competitive adsorption of SO_2 and NO_x on Nb–VO_x/CeO_2 and VO_x/CeO_2 catalysts, the DRIFT spectra of NO + O_2 + SO_2 adsorption were measured and are shown in Figure 6. After introducing SO_2 and NO_x, several

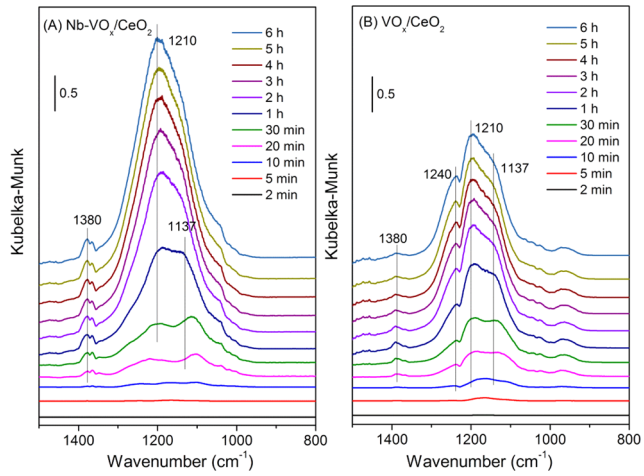

Figure 6. DRIFT spectra of 500 ppm of NO + 5 vol % O_2 + 100 ppm of SO_2 adsorption on Nb–VO_x/CeO_2 (A) and VO_x/CeO_2 (B) catalysts at 250 °C.

bands were detected on the samples. According to the literature,[16,33−35] the bands at 1210, 1240, and 1137, 1380 cm^{-1} were ascribed to nitrate and sulfate species, respectively. Initially, sulfate and nitrate formed simultaneously on Nb–VO_x/CeO_2. Their intensities increased with exposure time within the first 2 h. Then the intensities of nitrate continued to increase, while the sulfate species decreased with the increase of reaction time. After 6 h of adsorption, the main species on Nb–VO_x/CeO_2 was nitrate. The amount of sulfate species on Nb–VO_x/CeO_2 was much smaller than that of nitrate species. However, sulfate existed on the VO_x/CeO_2 surface at all times, and less nitrate formed on it than that on Nb–VO_x/CeO_2. In the presence of NO_x and SO_2, the Nb–VO_x/CeO_2 catalyst mainly adsorbed NO_x and was covered with nitrate, while VO_x/CeO_2 coadsorbed nitrate and sulfate and formed less nitrate.

Figure S6 (SI) showed the NH_3-SCR activity over Nb–VO_x/CeO_2 after sulfation for 48 h in the presence of NO and in the presence of NH_3. Both of these samples presented low activity, similar to Nb–VO_x/CeO_2 sulfation by SO_2 + O_2 only. After a long time of sulfation in the presence of NO, the catalysts could be covered with sulfate due to its higher thermal stability than nitrate.

The DRIFTS of SO_2 adsorption on Nb–VO_x/CeO_2 and VO_x/CeO_2 are exhibited in Figure 7. After the introduction of SO_2 + O_2, several bands attributed to sulfate species were observed. The amount of sulfate on Nb–VO_x/CeO_2 was close to that on VO_x/CeO_2, in accordance with the XPS results of Nb–VO_x/CeO_2–sulfation by SO_2 + O_2 only and VO_x/CeO_2–sulfation by SO_2 + O_2 only. From Figures 6A and 7A, during the introduction of SO_2 + NO + O_2 and SO_2 + O_2, the main adsorption species were nitrate and sulfate on Nb–VO_x/CeO_2, respectively. This indicates that SO_2 and NO adsorb competitively on the same active sites on the surface of the catalyst, because both SO_2 and NO are acidic gases, in accordance with the published literature.[36] Over Nb–VO_x/CeO_2, the adsorption ability of NO on active sites was much higher than that of SO_2. However, the deposited sulfate species on VO_x/CeO_2 would occupy part of the active sites needed for NO adsorption as seen from Figures 6B and 7B.

The effect of sulfation by SO_2 + O_2 only on the NH_3-SCR reaction mechanism was also investigated. The DRIFT spectra of NH_3 adsorption on the fresh and sulfated Nb–VO_x/CeO_2

DOI: 10.1021/acs.jpcc.6b12772
J. Phys. Chem. C 2017, 121, 7803−7809

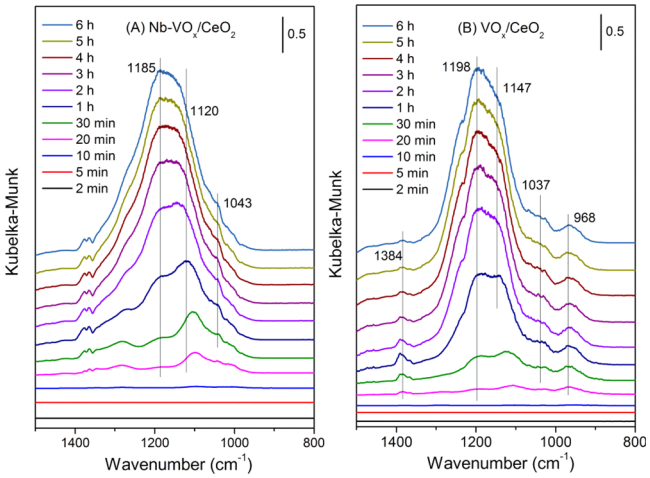

Figure 7. DRIFT spectra of 100 ppm of SO_2 + 5 vol % O_2 adsorption on Nb−VO_x/CeO_2 (A) and VO_x/CeO_2 (B) catalysts at 250 °C.

and VO_x/CeO_2 catalysts at 175 °C are shown in Figure 8A. After NH_3 adsorption and N_2 purging, these samples were

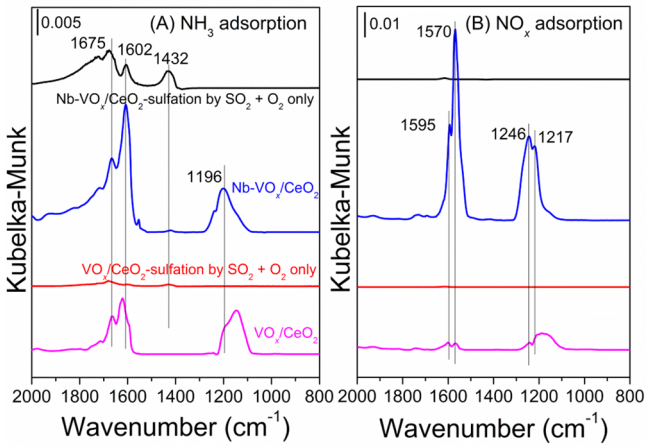

Figure 8. DRIFTS of 500 ppm of NH_3 adsorption (A) and 500 ppm of NO + 5 vol % O_2 adsorption (B) on fresh and sulfated Nb−VO_x/CeO_2 and VO_x/CeO_2 catalysts at 175 °C.

covered with various NH_3 species. The bands at 1675 and 1432 cm^{-1} were assigned to symmetric and asymmetric bending vibrations of ionic NH_4^+ bound to the Brønsted acid sites, and the bands at 1602 and 1196 cm^{-1} were attributed to asymmetric and symmetric bending vibrations of the N−H bonds in NH_3 coordinated to Lewis acid sites.[16,37,38] The Nb−VO_x/CeO_2 catalyst exhibited more acid sites than VO_x/CeO_2, including both Brønsted acid sites and Lewis acid sites. After sulfation by SO_2 + O_2 only, the amount of Lewis acid sites decreased significantly due to the formation of sulfate and the reduction of specific surface area. However, the formation of sulfate species resulted in more Brønsted acid sites per square meter on the catalyst. Therefore, Nb−VO_x/CeO_2−sulfation by SO_2 + O_2 only still presented Brønsted acid sites. The amount of acid sites on Nb−VO_x/CeO_2−sulfation by SO_2 + O_2 only was still larger than that on VO_x/CeO_2−sulfation by SO_2 + O_2 only, i.e., the same as the fresh samples.

Figure 8B shows the DRIFTS results of NO + O_2 adsorption on the fresh and sulfated Nb−VO_x/CeO_2 and VO_x/CeO_2 catalysts at 175 °C. After NO + O_2 adsorption and N_2 purge, the fresh Nb−VO_x/CeO_2 and VO_x/CeO_2 sample surfaces were covered with various nitrate species, including bidentate nitrate (1570 and 1246 cm^{-1}) and bridging nitrate (1595 and 1217 cm^{-1}).[33,39] The adsorption amount of NO_x on the fresh Nb−VO_x/CeO_2 catalyst was larger than that on the fresh VO_x/CeO_2. After sulfation by SO_2 + O_2 only, Nb−VO_x/CeO_2 and VO_x/CeO_2 both presented almost no nitrate species, due to the accumulation of sulfate on the samples and the reduction of specific surface area.

To investigate the reactivity of adsorbed NH_3 species in the SCR reaction, in situ DRIFT spectra of the reaction between NO + O_2 and preadsorbed NH_3 species on Nb−VO_x/CeO_2−sulfation by SO_2 + O_2 only and VO_x/CeO_2−sulfation by SO_2 + O_2 only were recorded as a function of time (Figure 9). After

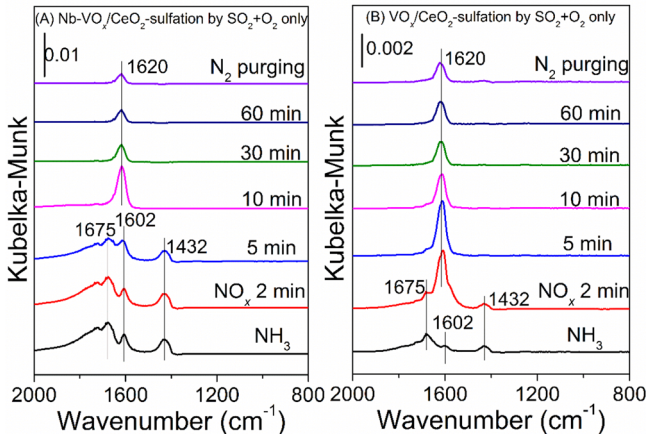

Figure 9. In situ DRIFT spectra of Nb−VO_x/CeO_2−sulfation by SO_2 + O_2 (A) and VO_x/CeO_2−sulfation by SO_2 + O_2 (B) pretreated by exposure to 500 ppm of NH_3 followed by exposure to 500 ppm of NO + 5 vol % O_2 at 175 °C.

NH_3 adsorption and N_2 purge, the sulfation sample surface was covered with various NH_3 species. When NO + O_2 was introduced to Nb−VO_x/CeO_2−sulfation by SO_2 + O_2 only, the intensity of the bands attributed to NH_3 adsorption species decreased gradually and disappeared after 10 min. Finally, only one band at 1620 cm^{-1}, which was ascribed to H_2O,[40,41] was observed, and no nitrate species formed on the surface of these samples. The adsorbed NH_3 species, including ionic NH_4^+ and coordinated NH_3, could both react with NO_x to form N_2 and H_2O. A similar phenomenon happened on VO_x/CeO_2−sulfation by SO_2 + O_2 only. The adsorbed NH_3 species on the sulfation samples could participate in the NH_3-SCR reaction.

4. DISCUSSION

The Nb−VO_x/CeO_2 catalyst exhibited higher NH_3-SCR activity than the VO_x/CeO_2 catalyst. After sulfation under SCR atmosphere, the NH_3-SCR activity over the Nb−VO_x/CeO_2 catalyst only decreased slightly, while the VO_x/CeO_2 catalyst showed much lower catalytic activity. From H_2-TPR and XPS results, only a small amount of sulfate formed on the Nb−VO_x/CeO_2−sulfation under SCR conditions sample. However, VO_x/CeO_2−sulfation under SCR conditions was covered with a considerable amount of sulfate and then presented a much smaller specific surface area than Nb−VO_x/CeO_2−sulfation under SCR conditions, leading to a reduction in the number of active sites. From the results of in situ

DOI: 10.1021/acs.jpcc.6b12772
J. Phys. Chem. C 2017, 121, 7803−7809

DRIFTS of NH_3 adsorption (Figure 8) and NH_3-TPD,[16] the amount of acid sites over Nb−VO_x/CeO_2 was remarkably larger than that over VO_x/CeO_2. The acidity of sulfate is stronger than that of nitrate. Therefore, the adsorption ability of NO on active sites was much higher than that of SO_2 on Nb−VO_x/CeO_2, in accordance with the published literature.[42] When introducing SO_2 + NO + O_2 simultaneously, Nb−VO_x/CeO_2 mainly adsorbed nitrate species, while VO_x/CeO_2 coadsorbed nitrate and sulfate. According to our published literature,[16] the adsorbed nitrate on Nb−VO_x/CeO_2 could participate in the NH_3-SCR reaction. The formation of sulfate, small specific surface area, and reduction in the number of active sites were responsible for the low catalytic activity over VO_x/CeO_2 after sulfation under SCR conditions. Nb−VO_x/CeO_2 preferentially adsorbed nitrate when sulfated under SCR conditions and thus still showed higher NH_3-SCR activity than the VO_x/CeO_2 sample.

After sulfation by SO_2 + O_2 only, Nb−VO_x/CeO_2 and VO_x/CeO_2 catalysts both exhibited low NH_3-SCR activity. A large amount of sulfate formed on the samples' surfaces, leading to a significant decrease in specific surface area. Therefore, the adsorption of NO_x was inhibited and the amount of acid sites was reduced. In our previous study,[16] the Langmuir−Hinshelwood mechanism existed for the NH_3-SCR over Nb−VO_x/CeO_2 at low temperatures, in which the adsorbed NO_x species reacted with adsorbed NH_3 to finally form N_2 and H_2O. The sulfation treatment inhibited the formation of nitrate species, so that the Langmuir−Hinshelwood reaction pathway was cut off. The NH_3-SCR reaction over the sulfated catalysts followed the Eley−Rideal mechanism, in which gaseous NO reacted with adsorbed NH_3 species to finally form N_2 and H_2O. Therefore, the low-temperature NH_3-SCR activity over Nb−VO_x/CeO_2−sulfation by SO_2 + O_2 only and VO_x/CeO_2−sulfation by SO_2 + O_2 only was much lower than that over the fresh catalysts.

5. CONCLUSIONS

The addition of Nb could enhance the NH_3-SCR activity and SO_2 tolerance over VO_x/CeO_2. The Nb−VO_x/CeO_2 catalyst exhibited excellent NH_3-SCR performance. After long-term SCR operation in a SO_2-containing atmosphere, the NO_x conversion over the VO_x/CeO_2 sample decreased more significantly than that over Nb−VO_x/CeO_2. According to the BET, H_2-TPR, XPS, and DRIFTs results, a large amount of sulfate was deposited on VO_x/CeO_2−sulfation under SCR conditions, resulting in a reduction in specific surface area and the number of active sites. Therefore, low SCR activity was obtained over VO_x/CeO_2 after sulfation in SCR. Nb−VO_x/CeO_2 adsorbed much more nitrate than sulfate when sulfated under SCR conditions, and then Nb−VO_x/CeO_2−sulfation under SCR conditions still showed much higher NH_3-SCR activity than VO_x/CeO_2−sulfation under SCR conditions. After sulfation by SO_2 + O_2 only, Nb−VO_x/CeO_2 and VO_x/CeO_2 catalysts both exhibited decreased NH_3-SCR activity. The sulfation process led to the formation of sulfate and the reduction of specific surface area, so that the active nitrate species could not form effectively. Therefore, the low-temperature SCR activity over Nb−VO_x/CeO_2−sulfation by SO_2 + O_2 only and VO_x/CeO_2−sulfation by SO_2 + O_2 only was inhibited due to the blocking of the Langmuir−Hinshelwood reaction pathway.

■ ASSOCIATED CONTENT

Supporting Information

The Supporting Information is available free of charge on the ACS Publications website at DOI: 10.1021/acs.jpcc.6b12772.

Figure S1 shows the effect of 300 ppm of SO_2 on SCR activity. Figure S2 shows NH_3-SCR activity over VO_x/CeO_2, Nb−VO_x/CeO_2 and Nb/CeO_2 catalysts. Figure S3 shows N_2 selectivity. Figure S4 and S5 present the NH_3-TPD and NO-TPD results, respectively. Figure S6 presents the NH_3-SCR activity over Nb−VO_x/CeO_2 after sulfation in the presence of NO and sulfation in the presence of NH_3 (PDF)

■ AUTHOR INFORMATION

Corresponding Author

*Fax: +86 592 6190990. Tel: +86 592 6190990. E-mail: hhe@iue.ac.cn.

ORCID

Zhihua Lian: 0000-0002-7413-180X

Wenpo Shan: 0000-0003-2818-5708

Present Address

‖F.L.: BASF Corp., 25 Middlesex Essex Turnpike, Iselin, NJ 08830, United States.

Notes

The authors declare no competing financial interest.

■ ACKNOWLEDGMENTS

This work was financially supported by the Natural Science Foundation of China (21607149), the Strategic Priority Research Program of the Chinese Academy of Sciences (XDB05050505), the Ministry of Science and Technology, China (2016YFC0205301), and the Natural Science Foundation of Fujian Province, China (2016J05142).

■ REFERENCES

(1) Qi, G. S.; Yang, R. T.; Chang, R. MnO_x-CeO_2 Mixed Oxides Prepared by Co-Precipitation for Selective Catalytic Reduction of NO with NH_3 at Low Temperatures. *Appl. Catal., B* **2004**, *51*, 93−106.

(2) Bosch, H.; Janssen, F. Formation and Control of Nitrogen Oxides. *Catal. Today* **1988**, *2*, 369−379.

(3) Huang, Z.; Zhu, Z.; Liu, Z.; Liu, Q. Formation and Reaction of Ammonium Sulfate Salts on V_2O_5/AC Catalyst During Selective Catalytic Reduction of Nitric Oxide by Ammonia at Low Temperatures. *J. Catal.* **2003**, *214*, 213−219.

(4) Busca, G.; Lietti, L.; Ramis, G.; Berti, F. Chemical and Mechanistic Aspects of the Selective Catalytic Reduction of NO_x by Ammonia over Oxide Catalysts: A Review. *Appl. Catal., B* **1998**, *18*, 1−36.

(5) Busca, G.; Larrubia, M. A.; Arrighi, L.; Ramis, G. Catalytic Abatement of NO_x: Chemical and Mechanistic Aspects. *Catal. Today* **2005**, *107−108*, 139−148.

(6) Boningari, T.; Pappas, D. K.; Ettireddy, P. R.; Kotrba, A.; Smirniotis, P. G. Influence of SiO_2 on Mitio(2) (M = Cu, Mn, and Ce) Formulations for Low-Temperature Selective Catalytic Reduction of NO_x with NH_3: Surface Properties and Key Components in Relation to the Activity of NO_x Reduction. *Ind. Eng. Chem. Res.* **2015**, *54*, 2261−2273.

(7) Dunn, J. P.; Koppula, P. R.; Stenger, H. G.; Wachs, I. E. Oxidation of Sulfur Dioxide to Sulfur Trioxide over Supported Vanadia Catalysts. *Appl. Catal., B* **1998**, *19*, 103−117.

(8) Balle, P.; Geiger, B.; Kureti, S. Selective Catalytic Reduction of NO_x by NH_3 on Fe/Hbea Zeolite Catalysts in Oxygen-Rich Exhaust. *Appl. Catal., B* **2009**, *85*, 109−119.

DOI: 10.1021/acs.jpcc.6b12772
J. Phys. Chem. C 2017, 121, 7803−7809

(9) Fang, C.; Zhang, D.; Shi, L.; Gao, R.; Li, H.; Ye, L.; Zhang, J. Highly Dispersed CeO_2 on Carbon Nanotubes for Selective Catalytic Reduction of NO with NH_3. *Catal. Sci. Technol.* **2013**, *3*, 803−811.
(10) Hu, P.; Huang, Z.; Hua, W.; Gu, X.; Tang, X. Effect of H_2O on Catalytic Performance of Manganese Oxides in NO Reduction by NH_3. *Appl. Catal., A* **2012**, *437-438*, 139−148.
(11) Xu, W.; He, H.; Yu, Y. Deactivation of a Ce/TiO_2 Catalyst by SO_2 in the Selective Catalytic Reduction of NO by NH_3. *J. Phys. Chem. C* **2009**, *113*, 4426−4432.
(12) Kijlstra, W. S.; Biervliet, M.; Poels, E. K.; Bliek, A. Deactivation by SO_2 of MnO_x-Al_2O_3 Catalysts Used for the Selective Catalytic Reduction of NO with NH_3 at Low Temperatures. *Appl. Catal., B* **1998**, *16*, 327−337.
(13) Notoya, F.; Su, C.; Sasaoka, E.; Nojima, S. Effect of SO_2 on the Low-Temperature Selective Catalytic Reduction of Nitric Oxide with Ammonia over TiO_2, ZrO_2, and Al_2O_3. *Ind. Eng. Chem. Res.* **2001**, *40*, 3732−3739.
(14) Luo, H. C.; Huang, B. C.; Fu, M. L.; Wu, J. L.; Ye, D. Q. SO_2 Deactivation Mechanism of Mnox/Mwcnts Catalyst for Low-Temperature Selective Catalytic Reduction of NO_x by Ammonia. *Acta Physchim. Sin.* **2012**, *28*, 2175−2182.
(15) Choo, S. T.; Yim, S. D.; Nam, I. S.; Ham, S. W.; Lee, J. B. Effect of Promoters Including WO_3 and BaO on the Activity and Durability of V_2O_5/Sulfated TiO_2 Catalyst for NO Reduction by NH_3. *Appl. Catal., B* **2003**, *44*, 237−252.
(16) Lian, Z.; Liu, F.; He, H.; Liu, K. Nb-Doped VO_x/CeO_2 Catalyst for NH_3-SCR of NO_x at Low Temperatures. *RSC Adv.* **2015**, *5*, 37675−37681.
(17) Lian, Z.; Liu, F.; He, H. Effect of Preparation Methods on the Activity of VO_x/CeO_2 Catalysts for the Selective Catalytic Reduction of NO_x with NH_3. *Catal. Sci. Technol.* **2015**, *5*, 389−396.
(18) Shen, M.; Wen, H.; Hao, T.; Yu, T.; Fan, D.; Wang, J.; Li, W.; Wang, J. Deactivation Mechanism of SO_2 on Cu/SAPO-34 NH_3-SCR Catalysts: Structure and Active Cu^{2+}. *Catal. Sci. Technol.* **2015**, *5*, 1741−1749.
(19) Casapu, M.; Kröcher, O.; Elsener, M. Screening of Doped MnO_x−CeO_2 Catalysts for Low-Temperature NO-SCR. *Appl. Catal., B* **2009**, *88*, 413−419.
(20) Yang, S. J.; Guo, Y. F.; Chang, H. Z.; Ma, L.; Peng, Y.; Qu, Z.; Yan, N. Q.; Wang, C. Z.; Li, J. H. Novel Effect of SO_2 on the SCR Reaction over CeO_2: Mechanism and Significance. *Appl. Catal., B* **2013**, *136-137*, 19−28.
(21) Zhang, L.; Li, L.; Cao, Y.; Yao, X.; Ge, C.; Gao, F.; Deng, Y.; Tang, C.; Dong, L. Getting Insight into the Influence of SO_2 on TiO_2/CeO_2 for the Selective Catalytic Reduction of NO by NH_3. *Appl. Catal., B* **2015**, *165*, 589−598.
(22) Huang, H.; Lan, Y.; Shan, W.; Qi, F.; Xiong, S.; Liao, Y.; Fu, Y.; Yang, S. Effect of Sulfation on the Selective Catalytic Reduction of NO with NH_3 over Gamma-Fe_2O_3. *Catal. Lett.* **2014**, *144*, 578−584.
(23) Yang, S.; Qi, F.; Liao, Y.; Xiong, S.; Lan, Y.; Fu, Y.; Shan, W.; Li, J. Dual Effect of Sulfation on the Selective Catalytic Reduction of NO with NH_3 over MnO_x/TiO_2: Key Factor of NH_3 Distribution. *Ind. Eng. Chem. Res.* **2014**, *53*, 5810−5819.
(24) Yang, S.; Guo, Y.; Yan, N.; Wu, D.; He, H.; Qu, Z.; Yang, C.; Zhou, Q.; Jia, J. Nanosized Cation-Deficient Fe-Ti Spinel: A Novel Magnetic Sorbent for Elemental Mercury Capture from Flue Gas. *ACS Appl. Mater. Interfaces* **2011**, *3*, 209−17.
(25) Yu, J.; Si, Z.; Chen, L.; Wu, X.; Weng, D. Selective Catalytic Reduction of NO_x by Ammonia over Phosphate-Containing $Ce_{0.75}Zr_{0.25}O_2$ Solids. *Appl. Catal., B* **2015**, *163*, 223−232.
(26) Shi, Y.; Shu, H.; Zhang, Y.; Fan, H.; Zhang, Y.; Yang, L. Formation and Decomposition of NH_4HSO_4 During Selective Catalytic Reduction of NO with NH_3 over V_2O_5-WO_3/TiO_2 Catalysts. *Fuel Process. Technol.* **2016**, *150*, 141−147.
(27) Song, L.; Chao, J.; Fang, Y.; He, H.; Li, J.; Qiu, W.; Zhang, G. Promotion of Ceria for Decomposition of Ammonia Bisulfate over V_2O_5-MoO_3/TiO_2 Catalyst for Selective Catalytic Reduction. *Chem. Eng. J.* **2016**, *303*, 275−281.
(28) Liu, F.; Asakura, K.; He, H.; Shan, W.; Shi, X.; Zhang, C. Influence of Sulfation on Iron Titanate Catalyst for the Selective Catalytic Reduction of NO_x with NH_3. *Appl. Catal., B* **2011**, *103*, 369−377.
(29) Gao, S.; Chen, X.; Wang, H.; Mo, J.; Wu, Z.; Liu, Y.; Weng, X. Ceria Supported on Sulfated Zirconia as a Superacid Catalyst for Selective Catalytic Reduction of NO with NH_3. *J. Colloid Interface Sci.* **2013**, *394*, 515−521.
(30) Liu, Z.; Su, H.; Chen, B.; Li, J.; Woo, S. Activity Enhancement of WO_3 Modified Fe_2O_3 Catalyst for the Selective Catalytic Reduction of NO_x by NH_3. *Chem. Eng. J.* **2016**, *299*, 255−262.
(31) Zhang, L.; Qu, H.; Du, T.; Ma, W.; Zhong, Q. H_2O and SO_2 Tolerance, Activity and Reaction Mechanism of Sulfated Ni-Ce-La Composite Oxide Nanocrystals in NH_3-SCR. *Chem. Eng. J.* **2016**, *296*, 122−131.
(32) Maqbool, M. S.; Pullur, A. K.; Ha, H. P. Novel Sulfation Effect on Low-Temperature Activity Enhancement of CeO_2-Added Sb-V_2O_5/TiO_2 Catalyst for NH_3-SCR. *Appl. Catal., B* **2014**, *152-153*, 28−37.
(33) Hadjiivanov, K. I. Identification of Neutral and Charged N_xO_y Surface Species by IR Spectroscopy. *Catal. Rev.: Sci. Eng.* **2000**, *42*, 71−144.
(34) Zhang, L.; Zou, W.; Ma, K.; Cao, Y.; Xiong, Y.; Wu, S.; Tang, C.; Gao, F.; Dong, L. Sulfated Temperature Effects on the Catalytic Activity of CeO_2 in NH_3-Selective Catalytic Reduction Conditions. *J. Phys. Chem. C* **2015**, *119*, 1155−1163.
(35) Liu, Z.; Zhang, S.; Li, J.; Zhu, J.; Ma, L. Novel V_2O_5-CeO_2/TiO_2 Catalyst with Low Vanadium Loading for the Selective Catalytic Reduction of NO_x by NH_3. *Appl. Catal., B* **2014**, *158-159*, 11−19.
(36) Wei, L.; Cui, S.; Guo, H.; Ma, X.; Zhang, L. DRIFT and DFT Study of Cerium Addition on SO_2 of Manganese-Based Catalysts for Low Temperature SCR. *J. Mol. Catal. A: Chem.* **2016**, *421*, 102−108.
(37) Zhang, L.; Pierce, J.; Leung, V. L.; Wang, D.; Epling, W. S. Characterization of Ceria's Interaction with NO_x and NH_3. *J. Phys. Chem. C* **2013**, *117*, 8282−8289.
(38) Lee, K. J.; Kumar, P. A.; Maqbool, M. S.; Rao, K. N.; Song, K. H.; Ha, H. P. Ceria Added Sb-V_2O_5/TiO_2 Catalysts for Low Temperature NH_3 SCR: Physico-Chemical Properties and Catalytic Activity. *Appl. Catal., B* **2013**, *142-143*, 705−717.
(39) Liu, C.; Chen, L.; Li, J.; Ma, L.; Arandiyan, H.; Du, Y.; Xu, J.; Hao, J. Enhancement of Activity and Sulfur Resistance of CeO_2 Supported on TiO_2-SiO_2 for the Selective Catalytic Reduction of NO by NH_3. *Environ. Sci. Technol.* **2012**, *46*, 6182−6189.
(40) Tso, T. L.; Lee, E. K. C. Role of Hydrogen Bonding Studied by the FTIR Spectroscopy of the Matrix-Isolated Molecular Complexes, Dimer of Water, Water.Carbon Dioxide, Water.Carbon Monoxide and Hydrogen Peroxide.N Carbon Monoxide in Solid Molecular Oxygen at 12−17 K. *J. Phys. Chem.* **1985**, *89*, 1612−1618.
(41) Goodman, A. L.; Bernard, E. T.; Grassian, V. H. Spectroscopic Study of Nitric Acid and Water Adsorption on Oxide Particles: Enhanced Nitric Acid Uptake Kinetics in the Presence of Adsorbed Water. *J. Phys. Chem. A* **2001**, *105*, 6443−6457.
(42) Zhou, H.; Su, Y.; Liao, W.; Deng, W.; Zhong, F. NO Reduction by Propane over Monolithic Cordierite-Based Fe/Al_2O_3 Catalyst: Reaction Mechanism and Effect of H_2O/SO_2. *Fuel* **2016**, *182*, 352−360.

DOI: 10.1021/acs.jpcc.6b12772
J. Phys. Chem. C 2017, 121, 7803−7809